

Neural Network based Interactive Lane Changing Planner in Dense Traffic with Safety Guarantee

Xiangguo Liu¹, Ruochen Jiao¹, Bowen Zheng², Dave Liang², Qi Zhu¹

Abstract— Neural network based planners have shown great promises in improving performance and task success rate in autonomous driving. However, it is very challenging to ensure safety of the system with learning enabled components, especially in dense and highly interactive traffic environments. In this work, we propose a neural network based lane changing planner framework that can ensure safety while sustaining system efficiency. To prevent too conservative planning, we assess the aggressiveness and identify the driving behavior of surrounding vehicles, then adapt the planned trajectory for the ego vehicle accordingly. The ego vehicle can proceed to change lanes if a safe evasion trajectory exists even in the worst case, otherwise, it can hesitate around current lateral position or return back to the original lane. We also quantitatively demonstrate the effectiveness of our planner design and its advantage over other baselines through extensive simulations with diverse and comprehensive experimental settings.

I. INTRODUCTION

Lane changing in dense traffic has been a challenging application in autonomous driving, especially in scenarios with complex inter-vehicle interactions. It is a common safety-efficiency dilemma. Some planners have larger buffer space [1] to handle uncertainties from surrounding vehicles and the environment, thus can be overly conservative and inefficient, while other planners put more emphasis on efficiency and task success rate, but safety is compromised. It is more challenging during the transition period to a fully-automated transportation system, because human-driven and autonomous vehicles need to interact with each other and share the transportation network. Without an accurate estimation of the other vehicle's intention, the lane changing process can be either inefficient or unsafe.

Neural network based machine learning techniques have been increasingly leveraged in autonomous driving for perception, prediction and planning. Compared with traditional rule-based planner, neural network based planner can greatly improve performance and has the potential to efficiently handle these near-accident scenarios [2], e.g., mandatory lane changing. However, the learning components also increase the difficulty in ensuring system safety. A large amount of neural network based methods [2], [3], [4], [5], [6], [7] measure system safety and performance by extensive simulations, which cannot provide safety guarantee. While

¹Xiangguo Liu, Ruochen Jiao and Qi Zhu are with the Department of Electrical and Computer Engineering, Northwestern University, Evanston, IL 60201, USA. xg.liu@u.northwestern.edu, ruochen.jiao@u.northwestern.edu, qzhu@northwestern.edu.

²Bowen Zheng and Dave Liang are with Pony.ai, Fremont, CA 94538, USA. bowen.zheng@pony.ai, dave.liang@pony.ai.

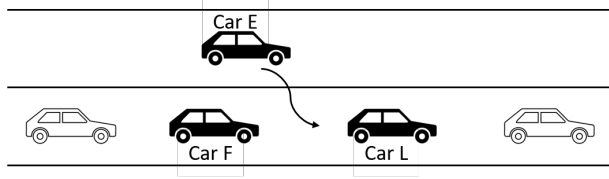


Fig. 1. Lane changing scenario.

the state-of-the-art safety verification techniques [8], [9], [10] can theoretically analyze learning-enabled systems, they are challenging to scale to high-dimensional systems and can result in conservative conclusions.

To overcome these challenges, we propose a neural network based planner design for highly interactive lane changing scenarios. More specifically, we have two neural network planners for longitudinal and lateral motions, respectively. The two planners take motion status of surrounding vehicles and the ego vehicle as input, and output planned accelerations for ego vehicle. In order to improve efficiency and ensure safety, the ego vehicle can make lane changing attempt under the neural network planners, as long as it has a safe evasion trajectory even in the worst case. If the safe evasion trajectory does not exist, the neural networks' planned trajectory will be adjusted according to safety analysis for all involved vehicles. To prevent an overly conservative planner design, we leverage another neural network to assess aggressiveness of the following vehicle in the target lane, thus predicting its behavior. In case that the following vehicle is collaborative, the ego vehicle can complete lane changing confidently, otherwise it needs to be cautious.

In this work, we are considering the scenario as shown in Fig. 1. The ego vehicle *E*, an autonomous vehicle, intends to change lanes and insert itself downstream of vehicle *F*, a human-driven or an autonomous vehicle in the target lane. We assume the worst case is that the leading vehicle *L* in the target lane decelerates abruptly, and at the same time the following vehicle *F* can accelerate and prevent ego vehicle *E* from cutting in. The future acceleration and behavior of the following vehicle *F* is predicted for safety analysis in the worst case. The evasion trajectory is considered to be safe if the ego vehicle can take it back to the original lane without colliding with other vehicles.

In summary, our work makes the following contributions:

- We propose a lane changing planner framework that can ensure safety even when the leading vehicle decelerates

abruptly and the following vehicle accelerates aggressively.

- We explicitly identify the behavior of the following vehicle to prevent too conservative planning while ensuring safety, which can improve lane changing success rate and efficiency, especially in dense traffic.
- We demonstrate the safety enhancement of our planner design through extensive simulations, compared with the naïve end2end neural network planner.

The rest of this paper is organized as follows. In Section II, we review related works on lane changing, inter-vehicle interaction and neural network based methods. In Section III, we demonstrate our planner design framework. We then present and analyze the experimental results in Section IV. We summarize the takeaways in Section V.

II. RELATED WORK

There are a rich literature of trajectory planning, and more specifically, lane changing, which is reviewed in detail in [11], [12], [13]. [14] proposes a dynamic lane changing planner, which can update its reference trajectory periodically. If necessary, it can plan a trajectory back to the original lane to eliminate collision. Similarly, [15] can plan a safe evasion trajectory. However, [14], [15] assume that the leading and following vehicles in the target lane will remain their velocities when the ego vehicle changes lanes, which may not hold due to the fluctuations of traffic stream and interactions between vehicles. [16] leverages dynamic programming to compute acceleration and timing to safely merge or change lanes, but the computation efficiency will be significantly influenced if we increase the discretization precision.

To improve efficiency and lane changing success rate, especially in dense traffic, prior works [17], [18], [19] have emphasized the importance of modelling inter-vehicle interactions. [17] proposes a game theory based lane changing model for connected vehicles, and calibrates different parameters in the utility functions for mandatory and discretionary lane changing scenarios. [20] assumes vehicles are all connected and cooperative, which is not satisfied in the transition period. [21] leverages partially observable Markov decision process to model the level of cooperation of other drivers, and incorporates this belief into reinforcement learning based planner for higher merging success rate. [22] uses RNN to model interaction between vehicles, then the predicted results will be incorporated in safety constraints of the MPC planner. [18] obtains a probability distribution of different intentions of surrounding vehicles by Bayesian estimation, then plans trajectories considering uncertain interactions with surrounding vehicles. In this work, we leverage a neural network to predict the accelerations of the following vehicle assuming it is collaborative or not. By comparing the prediction with its true acceleration, we can identify its behavior. For those predictions with low confidence, the following vehicle is assumed to be aggressive, such that the ego vehicle can remain safe in the worst case.

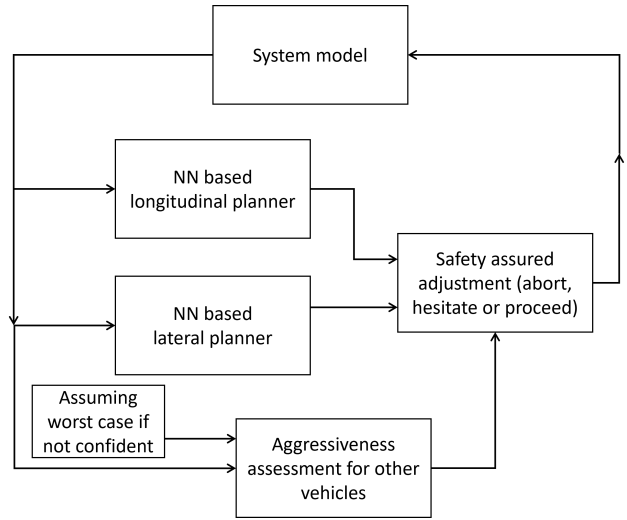


Fig. 2. Planner design framework.

Machine learning techniques are increasingly popular in this challenging application. [23] leverages reinforcement learning and considers the possible action of aborting lane changing and return back to original lane. [24] develops hierarchical reinforcement learning based planners to address both of the timing and maneuver for lane changing. [25], [26] are also based on reinforcement learning. [2] proposes a hierarchical reinforcement and imitation learning (H-REIL) approach that consists of low-level policies learned by imitation learning under different driving modes, and a high-level policy learned by reinforcement learning that switches between driving modes. However, all these methods cannot ensure safety.

[27] analyzes the distance between vehicles to ensure safety for lane changing, which is derived only based on the braking capability. Without considering steering, the distance is conservative, thus is hard to be satisfied, especially in dense traffic. Moreover, it does not explicitly analyze the intention of following vehicle. This limitation also exists in [28], [29]. Our method to analyze safety is closely related to [30]. It analyzes the minimum critical distance around surrounding vehicles by considering braking and steering capabilities, respectively. It assumes the worst case is that the leading vehicle has a fully stop suddenly or the following vehicle remains its acceleration to close the gap. However, it neglects the fact that ego vehicle can steer and brake at the same time to avoid collision. Also the worst case assumptions for the leading and following vehicle can happen at the same time. To avoid collision with both vehicles, the ego vehicle could accelerate or decelerate depending on the relative positions. [30] does not have the discussion, nor does it consider inter-vehicle interactions.

III. PLANNER DESIGN WITH SAFETY GUARANTEE

Our planner design is shown in Fig. 2. In this framework, we develop neural network based planners for longitudinal and lateral motion planning. We present the details in Section III-A. To improve lane changing success rate in dense

TABLE I
INPUT AND OUTPUT OF NEURAL NETWORK BASED PLANNER

notation	definition
input	
p_x	longitudinal position of the ego vehicle
p_y	lateral position of the ego vehicle
v_x	longitudinal velocity of the ego vehicle
v_y	lateral velocity of the ego vehicle
$p_{x,l}$	longitudinal position of the leading vehicle in the target lane
$v_{x,l}$	longitudinal velocity of the leading vehicle in the target lane
$p_{x,f}$	longitudinal position of the following vehicle in the target lane
$v_{x,f}$	longitudinal velocity of the following vehicle in the target lane
output	
a_x	longitudinal acceleration of the ego vehicle
a_y	lateral acceleration of the ego vehicle

traffic, we leverage another neural network to assess aggressiveness of the following vehicle F , which is addressed in Section III-B. According to the identified behavior of vehicle F , we conduct safety analysis and compute the critical region to avoid collision in the worst case. The trajectory planned under neural networks is adjusted in advance if there is any possibility of collision during the lane changing process, which is elaborated in Section III-C.

A. Longitudinal and Lateral Planners

The neural network has seven input variables¹ and two output variables, as summarized in table I. In order to cover as much as traffic scenarios as possible, we synthesis the dataset by simulations. We uniformly sample the initial status of the system by following $0 \leq p_{x,l} - p_x \leq 50$ m, $30 \leq p_{x,l} - p_{x,f} \leq 80$ m, $20 \text{ m/s} \leq v_x \leq 30 \text{ m/s}$ and $25 \text{ m/s} \leq v_{x,f} \leq 35 \text{ m/s}$. Additionally, the ego vehicle initially is at the center of the original lane and has no lateral speed. Then we let the leading vehicle remain its velocity $v_{x,l} = 30$ meters per second for the next $t_h = 10$ seconds. The ego vehicle changes lanes under an optimal controller [31] with step size $\delta t = 0.1$ seconds. The optimal controller is minimizing fuel consumption and lane changing time while satisfying safety and comfort constraints. More details can be found in [31].

The dataset collects system states and accelerations of the ego vehicle at every step, which composed of about 871 thousand entries. The neural network planner is trained to minimize mean squared error with Adam optimizer. It is noted that with human driving dataset or other methods to synthesis dataset, the planner may be different, but the framework will always ensure system safety.

B. Aggressiveness Assessment and Behavior Identification

According to [32], the driving behavior of the following vehicle follows one model when it is collaborative and another model when it is aggressive. This assumption is validated by real-world human driving data. In this work, we have similar assumptions. We assume the following vehicle F follows the ego vehicle E when it is collaborative and follows the leading vehicle L when it is aggressive. The underlying

¹There are eight input variables in table I. However, among p_x , $p_{x,l}$ and $p_{x,f}$, only two of them are independent.

car following model is Intelligent Driver Model (IDM) [33], as formulated below:

$$a_{x,f} = a_{x,a} \left[1 - \left(\frac{v_{x,f}}{v_m} \right)^4 - \left(\frac{h_s + t_g v_{x,f} - \dot{h} v_{x,f} / \sqrt{4 a_{x,a} a_{x,d}}}{h} \right)^2 \right] \quad (1)$$

where $a_{x,f}$ is acceleration of the following vehicle, $a_{x,a}$ is maximum acceleration, $v_{x,f}$ is velocity of the following vehicle, v_m is maximum velocity, t_g is desired time headway, $a_{x,d}$ is maximum braking deceleration. h is headway and depends on whether the following vehicle is collaborative or not.

$$h = \begin{cases} p_x - p_{x,f} & \text{if vehicle } F \text{ is collaborative} \\ p_{x,l} - p_{x,f} & \text{otherwise} \end{cases} \quad (2)$$

For both two cases, we leverage a neural network to predict the accelerations of the following vehicle. Let a_1 and a_0 denote the accelerations when it is collaborative or aggressive, respectively. Different from the motion planner, we do not need p_y and v_y as input variables of the neural network.

For this prediction task, we also synthesis the dataset by simulations. We generate all kinds of traffic states of the three vehicles and compute the accelerations of the following vehicle F with IDM model. The parameters in the IDM model are uniformly sampled by following $a_{x,a} = 4 \text{ m/s}^2$, $v_m = \dot{h} + v_{x,f}$, $5 \leq h_s \leq 8$ m, $1 \leq t_g \leq 2$ s, $a_{x,d} = 6 \text{ m/s}^2$. With the dataset of one million entries, we train the neural network to minimize mean squared error with Adam optimizer.

The following vehicle's behavior is identified by comparing its true acceleration $a_{x,f}^*$ with predicted a_1 and a_0 . When $a_{x,f}^*$ is closer to a_1 , the following vehicle F is collaborative and follows the ego vehicle E ; when $a_{x,f}^*$ is closer to a_0 , it is aggressive and follows the leading vehicle L .

$$\begin{cases} |a_{x,f}^* - a_1| < |a_{x,f}^* - a_0| - a_{th} \\ \rightarrow \text{vehicle } F \text{ is collaborative} \\ |a_{x,f}^* - a_0| < |a_{x,f}^* - a_1| - a_{th} \\ \rightarrow \text{vehicle } F \text{ is aggressive} \\ -a_{th} \leq |a_{x,f}^* - a_0| - |a_{x,f}^* - a_1| \leq a_{th} \\ \rightarrow \text{uncertain} \end{cases} \quad (3)$$

where a_{th} is a threshold. The larger a_{th} , the higher confidence on the behavior prediction. For those uncertain scenarios, we still assume vehicle F is aggressive such that planned trajectory for ego vehicle is conservative and safe.

Based on the predicted behavior of the following vehicle, we conduct safety analysis. We assume that (1) if the following vehicle is collaborative and willing to create gap for ego vehicle, it can at least decelerate with $a_{x,f,d} = 6 \text{ m/s}^2$. (2) if the following vehicle is aggressive, in the worst case, it can accelerate with $a_{x,f,a} = 4 \text{ m/s}^2$ to prevent ego vehicle from cutting in.

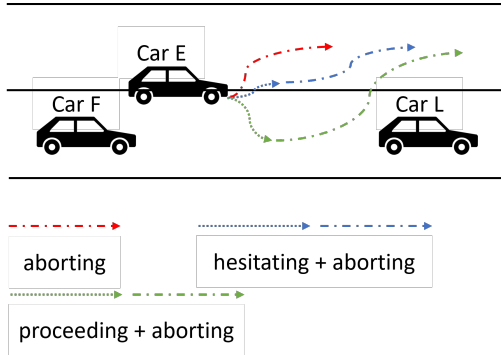


Fig. 3. At every step in the lane changing process, the ego vehicle has three strategy choices. The first is proceeding to change lanes, in which case the short-term proceeding trajectory (green dotted line) and following complete aborting trajectory (green dash-dotted line) should be verified with safety guarantee. If the first strategy is not safe, the ego vehicle can hesitate around current lateral position, and we need to verify safety for the short-term hesitating trajectory (blue dotted line) and following complete aborting trajectory (blue dash-dotted line). If both strategies do not work, the ego vehicle can directly abort lane changing behavior and go back to the original lane (red dash-dotted line), which is already verified to be safe in last planning step.

C. Safety Analysis and Motion Adjustment

We assume the ego vehicle is safe when it is in the original lane at the very beginning. At every step during lane changing, the ego vehicle has a safe evasion trajectory computed at last step. As shown in Fig. 3, it has three options with strictly decreasing preference: proceed changing lane, hesitate around current lateral position or abort changing lane and return back to the original lane. It analyzes the state after executing selected behavior for one time step. If it has a safe evasion trajectory following that, it can go ahead with the selected behavior; otherwise, it has to attempt a less preferred behavior. In summary, we ensure the safety of the ego vehicle by only selecting the strategy with a following safe evasion trajectory.

The behavior of proceeding changing lane is to directly follow the longitudinal and lateral accelerations computed using the neural network planners. For hesitating, the lateral acceleration is adjusted to diminish the velocity soon:

$$a_y = \min(\max(-v_y/\delta t, -a_{y,m}), a_{y,m}) \quad (4)$$

where $a_{y,m}$ is the absolute value of maximal lateral acceleration.

Next we will present the safe evasion trajectory. The optimal lateral motion is to return back to the original lane as soon as possible. We define time $t = 0$ when the ego vehicle just starts taking the evasion trajectory. The centers of the original and target lane are $y = 0$ and $y = w_l$, respectively. The width of a vehicle is denoted as w_v . The ego vehicle is completely in the original lane when $p_y \leq \frac{w_l - w_v}{2}$. As shown in Fig. 4, the fastest lateral motion is represented as the black solid line. The ego vehicle has lateral acceleration $a_y = -a_{y,m}$ when $t \in [0, t_1]$ and then $a_y = a_{y,m}$ when $t \in [t_1, t_{y,f}]^2$, finally

²Here $t_{y,f}$ equals t^1 in Fig. 4, in which we use t^1 , t^2 and t^3 for convenient explanation.

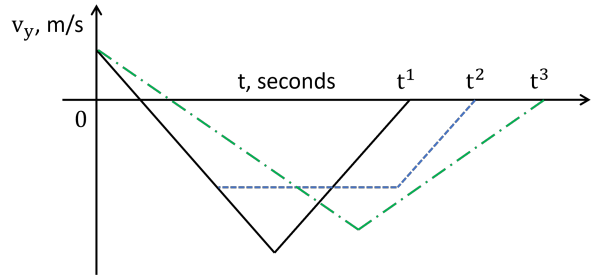


Fig. 4. The black solid line represents that the ego vehicle first decelerates and then accelerates laterally with maximum acceleration $a_{y,m}$. It reaches $p_y = \frac{w_l - w_v}{2}$ and $v_y = 0$ at t^1 . The blue dash line represents that the ego vehicle first decelerates, then keeps the negative velocity and finally accelerates, and it cost time t^2 . The green dot dash line represents a similar pattern as the black solid line, except that the ego vehicle uses a smaller lateral acceleration. It takes t^3 to return back to the original lane.

it reaches the position $p_y = \frac{w_l - w_v}{2}$ with $v_y = 0$.

$$\begin{cases} p_{y,t_0} + v_{y,t_0}t_1 - \frac{a_{y,m}t_1^2}{2} + (v_{y,t_0} - a_{y,m}t_1)(t_{y,f} - t_1) \\ + \frac{a_{y,m}(t_{y,f} - t_1)^2}{2} = \frac{w_l - w_v}{2} \\ v_{y,t_0} - a_{y,m}t_1 + a_{y,m}(t_{y,f} - t_1) = 0 \end{cases} \quad (5)$$

where p_{y,t_0} and v_{y,t_0} are the lateral position and velocity of the ego vehicle when $t = 0$.

By solving Eq. 5, we acquire

$$\begin{cases} t_1 = \frac{v_{y,t_0}}{a_{y,m}} + \sqrt{\frac{p_{y,t_0}}{a_{y,m}} + \frac{v_{y,t_0}^2}{2a_{y,m}^2} - \frac{w_l - w_v}{2a_{y,m}}} \\ t_{y,f} = \frac{v_{y,t_0}}{a_{y,m}} + 2\sqrt{\frac{p_{y,t_0}}{a_{y,m}} + \frac{v_{y,t_0}^2}{2a_{y,m}^2} - \frac{w_l - w_v}{2a_{y,m}}} \end{cases} \quad (6)$$

In cases that $t_1 < 0$, the ego vehicle should get rid of the decelerating process and keep accelerating when $t \in [0, t_{y,f}]$.

$t_{y,f}$ is also modified to $t_{y,f} = -\frac{v_{y,t_0}}{a_{y,m}} - \sqrt{-\frac{2p_{y,t_0}}{a_{y,m}} + \frac{v_{y,t_0}^2}{a_{y,m}^2} + \frac{w_l - w_v}{a_{y,m}}}$.

In other cases that the square root $\sqrt{\frac{p_{y,t_0}}{a_{y,m}} + \frac{v_{y,t_0}^2}{2a_{y,m}^2} - \frac{w_l - w_v}{2a_{y,m}}}$ has no real value solution, which indicates $p_{y,t_0} < \frac{w_l - w_v}{2}$. If $v_{y,t_0} \leq 0$, it is completely in the original lane and even not moving towards the target lane. If $v_{y,t_0} > 0$, the ego vehicle just need to decelerate until $v_y = 0$, and it remains in the original lane.

We assume the ego vehicle E , leading vehicle L and following vehicle F all have the same maximal longitudinal acceleration $a_{x,a} = a_{x,l,a} = a_{x,f,a}$ and braking deceleration $a_{x,d} = a_{x,l,d} = a_{x,f,d}$. Let p_{x,t_0} and v_{x,t_0} represent the longitudinal position and velocity of the ego vehicle when $t = 0$, respectively. For simplicity of notation, we omit the subscript of t_0 , and use $p_{x,l}$, $v_{x,l}$, $p_{x,f}$ and $v_{x,f}$ to denote the longitudinal position and velocity of the leading and following vehicles when $t = 0$, respectively. Next we will temporarily neglect the following vehicle F , and analyze the longitudinal motion when the leading vehicle L decelerates with $a_{x,l,d}$ abruptly.

If $v_{x,l} \geq v_{x,t_0}$, then $\frac{v_{x,l}^2}{2a_{x,l,d}} \geq \frac{v_{x,t_0}^2}{2a_{x,d}}$, the ego vehicle can prevent collisions with the leading vehicle if it decelerates with $a_{x,d}$. If $v_{x,l} < v_{x,t_0}$, the ego vehicle takes at least $t_{x,f} = \frac{v_{x,t_0}}{a_{x,d}}$ to fully stop. If $t_{x,f} \geq t_{y,f}$, ego vehicle only needs to keep

enough headway when $t \in [0, t_{y,f}]$ because it is already not in the target lane when $t \in [t_{y,f}, t_{x,f}]$. We define C_1 to reflect the minimum headway³:

$$C_1 = \begin{cases} p_{x,t_0} - p_{x,l} + v_{x,t_0} t_{y,f} - \frac{a_{x,d} t_{y,f}^2}{2} - \frac{v_{x,l}^2}{2a_{x,l,d}} + p_m & \text{if } \frac{v_{x,l}}{a_{x,l,d}} < t_{y,f} \\ p_{x,t_0} - p_{x,l} + (v_{x,t_0} - v_{x,l}) t_{y,f} - \frac{(a_{x,d} - a_{x,l,d}) t_{y,f}^2}{2} + p_m & \text{otherwise} \end{cases} \quad (7)$$

where p_m is the minimum gap between vehicles to avoid collisions. We need $C_1 < 0$ to ensure safety. If $t_{x,f} < t_{y,f}$, ego vehicle needs to keep enough headway when $t \in [0, t_{x,f}]$. Similarly, we define C_2 and need $C_2 < 0$ to ensure safety.

$$C_2 = p_{x,t_0} - p_{x,l} + \frac{v_{x,t_0}^2}{2a_{x,d}} - \frac{v_{x,l}^2}{2a_{x,l,d}} + p_m \quad (8)$$

Next we assume at the same time, the following vehicle F accelerates to prevent ego vehicle from cutting in. In such case, the ego vehicle can even accelerate and get closer to the leading vehicle, thus acquiring more time for lateral evasion before the following vehicle catches up. As shown in Fig. 5, the black solid line represents a longitudinal velocity curve of the ego vehicle corresponding that it first accelerates with $a_{x,a}$, then decelerates with $a_{x,d}$. The blue dash line and green dot dash line represent other two possible velocity curves. Let p_x^1 , p_x^2 and p_x^3 denote the position of the ego vehicle following the three velocity curves, respectively. If the position (and headway) of the ego vehicle at $t = t_{y,f}$ following the three curves are the same, i.e., $p_{x,t_{y,f}}^1 = p_{x,t_{y,f}}^2 = p_{x,t_{y,f}}^3$, the black solid line can result in the smallest headway when $t \in [0, t_{y,f}]$. In other words, it is the fastest longitudinal motion to get closer to the leading vehicle. Lastly, the ego vehicle needs to keep enough headway.

We assume the ego vehicle accelerates with $a_x = a_{x,a}$ when $t \in [0, t_2]$ and then decelerates with $a_x = -a_{x,d}$ until it stops when $t \in [t_2, t_{y,f}]$. If $\frac{v_{x,t_0}}{a_{x,d}} \geq t_{y,f}$, we have

$$\begin{cases} p_{x,t_0} + v_{x,t_0} t_2 + \frac{a_{x,a} t_2^2}{2} + (v_{x,t_0} + a_{x,a} t_2)(t_{y,f} - t_2) \\ - \frac{a_{x,d} (t_{y,f} - t_2)^2}{2} - p_{x,l} - \frac{v_{x,l}^2}{2a_{x,l,d}} + p_m = 0 \\ \text{if } \frac{v_{x,l}}{a_{x,l,d}} < t_{y,f} \\ p_{x,t_0} + v_{x,t_0} t_2 + \frac{a_{x,a} t_2^2}{2} + (v_{x,t_0} + a_{x,a} t_2)(t_{y,f} - t_2) \\ - \frac{a_{x,d} (t_{y,f} - t_2)^2}{2} - p_{x,l} - v_{x,l} t_{y,f} + \frac{a_{x,l,d} t_{y,f}^2}{2} + p_m = 0 \\ \text{otherwise} \end{cases} \quad (9)$$

³It is indeed a constant minus the minimum headway.

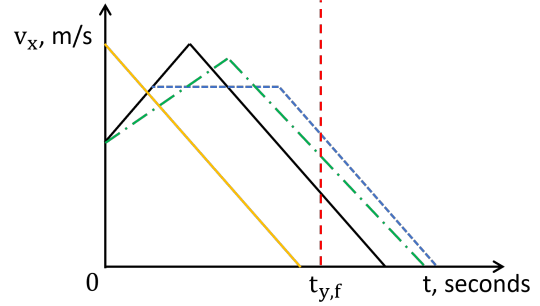


Fig. 5. The yellow solid line represents the velocity curve of the leading vehicle, which decelerates abruptly. The black solid line represents a possible longitudinal velocity curve of the ego vehicle. It first accelerates with $a_{x,a}$, then decelerates with $a_{x,d}$. It is at $t = t_{y,f}$ that the ego vehicle is the closest to leading vehicle when $t \in [0, t_{y,f}]$. We are not interested in the velocity curve when $t > t_{y,f}$ because ego vehicle is already not in the target lane. Other possible velocity curves of the ego vehicle are represented by the blue dash line and green dot dash line. The blue dash line corresponds that it first accelerates, then keeps the velocity and finally decelerates; the green dot dash line represents that its acceleration and deceleration are smaller than $a_{x,a}$ and $a_{x,d}$.

In other cases that $\frac{v_{x,t_0}}{a_{x,d}} < t_{y,f}$, we have

$$\begin{cases} p_{x,t_0} + v_{x,t_0} t_2 + \frac{a_{x,a} t_2^2}{2} + \frac{(v_{x,t_0} + a_{x,a} t_2)^2}{2a_{x,d}} \\ - p_{x,l} - \frac{v_{x,l}^2}{2a_{x,l,d}} + p_m = 0 \\ \text{if } t_2 + \frac{v_{x,t_0} + a_{x,a} t_2}{a_{x,d}} < t_{y,f} \\ p_{x,t_0} + v_{x,t_0} t_2 + \frac{a_{x,a} t_2^2}{2} + (v_{x,t_0} + a_{x,a} t_2)(t_{y,f} - t_2) \\ - \frac{a_{x,d} (t_{y,f} - t_2)^2}{2} - p_{x,l} - \frac{v_{x,l}^2}{2a_{x,l,d}} + p_m = 0 \\ \text{otherwise} \end{cases} \quad (10)$$

where $t_2 + \frac{v_{x,t_0} + a_{x,a} t_2}{a_{x,d}} < t_{y,f}$ corresponds that the ego vehicle gets $v_{x,t} = 0$ before $t = t_{y,f}$.

By solving Eq. 9 and 10 and substituting Eq. 7 and 8, we get

$$t_2 = \begin{cases} C_3 = -\frac{v_{x,t_0}}{a_{x,a}} + \sqrt{\frac{v_{x,t_0}^2}{a_{x,a}^2} - \frac{2a_{x,d} C_2}{a_{x,a}(a_{x,a} + a_{x,d})}} \\ \text{if } C_3 + \frac{v_{x,t_0} + a_{x,a} C_3}{a_{x,d}} < t_{y,f} \\ t_{y,f} - \sqrt{t_{y,f}^2 + \frac{2C_1}{a_{x,a} + a_{x,d}}} \\ \text{otherwise} \end{cases} \quad (11)$$

If $\sqrt{t_{y,f}^2 + \frac{2C_1}{a_{x,a} + a_{x,d}}}$ has no real value solution, that means ego vehicle can keep accelerating and still remain enough gap with leading vehicle when $t \in [0, t_{y,f}]$.

To prevent collisions with the following vehicle accelerat-

ing with $a_{x,f,a}$, we have

$$\left\{ \begin{array}{l} p_{x,t_0} + v_{x,t_0}t_2 + \frac{a_{x,a}t_2^2}{2} + \frac{(v_{x,t_0} + a_{x,a}t_2)^2}{2a_{x,d}} \\ -p_{x,f} - v_{x,f}t_{y,f} - \frac{a_{x,f,a}t_{y,f}^2}{2} - p_m > 0 \\ \quad \text{if } t_2 + \frac{v_{x,t_0} + a_{x,a}t_2}{a_{x,d}} < t_{y,f} \\ p_{x,t_0} + v_{x,t_0}t_2 + \frac{a_{x,a}t_2^2}{2} + (v_{x,t_0} + a_{x,a}t_2)(t_{y,f} - t_2) \\ -\frac{a_{x,d}(t_{y,f} - t_2)^2}{2} - p_{x,f} - v_{x,f}t_{y,f} - \frac{a_{x,f,a}t_{y,f}^2}{2} - p_m > 0 \\ \quad \text{otherwise} \end{array} \right. \quad (12)$$

Another case is that following vehicle is collaborative, willing to decelerate and create gap for ego vehicle. If $v_{x,f} \leq v_{x,t_0}$, the following vehicle always has enough space to avoid collisions. If $v_{x,f} > v_{x,t_0}$ and $v_{x,f} - a_{x,f,d}t_2 \leq v_{x,t_0} + a_{x,a}t_2$, we need

$$p_{x,t_0} - p_{x,f} - p_m - \frac{(a_{x,f,d} + a_{x,a})}{2} \left(\frac{v_{x,f} - v_{x,t_0}}{a_{x,f,d} + a_{x,a}} \right)^2 > 0 \quad (13)$$

If $v_{x,f} - a_{x,f,d}t_2 > v_{x,t_0} + a_{x,a}t_2$, then

$$\left\{ \begin{array}{l} p_{x,t_0} + v_{x,t_0}t_2 + \frac{a_{x,a}t_2^2}{2} + \frac{(v_{x,t_0} + a_{x,a}t_2)^2}{2a_{x,d}} \\ -p_{x,f} - \frac{v_{x,f}^2}{2a_{x,f,d}} - p_m > 0 \\ \quad \text{if } \frac{v_{x,f}}{a_{x,f,d}} < t_{y,f} \\ p_{x,t_0} + v_{x,t_0}t_2 + \frac{a_{x,a}t_2^2}{2} + \frac{(v_{x,t_0} + a_{x,a}t_2)^2}{2a_{x,d}} \\ -p_{x,f} - v_{x,f}t_{y,f} + \frac{a_{x,f,d}t_{y,f}^2}{2} - p_m > 0 \\ \quad \text{else if } t_2 + \frac{v_{x,t_0} + a_{x,a}t_2}{a_{x,d}} < t_{y,f} \\ p_{x,t_0} + v_{x,t_0}t_2 + \frac{a_{x,a}t_2^2}{2} + (v_{x,t_0} + a_{x,a}t_2)(t_{y,f} - t_2) \\ -\frac{a_{x,d}(t_{y,f} - t_2)^2}{2} - p_{x,f} - v_{x,f}t_{y,f} + \frac{a_{x,f,d}t_{y,f}^2}{2} - p_m > 0 \\ \quad \text{otherwise} \end{array} \right. \quad (14)$$

Generally, if the acceleration of following vehicle can be any value in a range, i.e., $a_{x,f} \in [-a_{x,f,d}, a_{x,f,a}]$. To ensure safety, we need to have

$$\left\{ \begin{array}{l} p_{x,t_0} + v_{x,t_0}t + \frac{a_{x,a}t^2}{2} \\ -p_{x,f} - v_{x,f}t - \frac{a_{x,f}t^2}{2} - p_m > 0 \\ \quad \text{if } t \in [0, t_2] \\ p_{x,t_0} + v_{x,t_0}t_2 + \frac{a_{x,a}t_2^2}{2} + (v_{x,t_0} + a_{x,a}t_2)(t - t_2) \\ -\frac{a_{x,d}(t - t_2)^2}{2} - p_{x,f} - v_{x,f}t - \frac{a_{x,f}t^2}{2} - p_m > 0 \\ \quad \text{else if } t \in [t_2, t_{y,f}], v_{x,f} + a_{x,f}t \geq 0 \\ \quad \text{and } (v_{x,t_0} + a_{x,a}t_2) - a_{x,d}(t - t_2) \geq 0 \\ p_{x,t_0} + v_{x,t_0}t_2 + \frac{a_{x,a}t_2^2}{2} + \frac{(v_{x,t_0} + a_{x,a}t_2)^2}{2a_{x,d}} \\ -p_{x,f} - v_{x,f}t - \frac{a_{x,f}t^2}{2} - p_m > 0 \\ \quad \text{else if } t \in [t_2, t_{y,f}], v_{x,f} + a_{x,f}t \geq 0 \\ \quad \text{and } (v_{x,t_0} + a_{x,a}t_2) - a_{x,d}(t - t_2) < 0 \\ p_{x,t_0} + v_{x,t_0}t_2 + \frac{a_{x,a}t_2^2}{2} + (v_{x,t_0} + a_{x,a}t_2)(t - t_2) \\ -\frac{a_{x,d}(t - t_2)^2}{2} - p_{x,f} - \frac{v_{x,f}^2}{2a_{x,f}} - p_m > 0 \\ \quad \text{otherwise} \end{array} \right. \quad (15)$$

TABLE II
PERFORMANCE OF BEHAVIOR IDENTIFICATION

	$a_{th} = 0$	$a_{th} = 0.15$	$a_{th} = 0.25$	$a_{th} = 0.5$	$a_{th} = 1$
easy					
uncertain rate	0%	2.28%	4.05%	9.16%	19.3%
error rate	4.61%	3.6%	3.05%	2.01%	0.91%
medium					
uncertain rate	0%	18.38%	31.33%	56.32%	79.65%
error rate	36.73%	28.82%	24.53%	15.87%	7.16%
hard					
uncertain rate	0%	65.26%	74.16%	85.57%	94.39%
error rate	49.76%	17.18%	12.76%	7.1%	2.74%

In summary, if the following vehicle F is aggressive and Eq. 12 is satisfied, or the following vehicle is collaborative and Eq. 13 and 14 are satisfied, the system is safe even in the worst case.

IV. EXPERIMENTAL RESULTS

In this section, we first present the performance of behavior identification for the following vehicle. Then we demonstrate the effectiveness of the complete planner framework, compared with the one with only neural network planners. In this paper, we refer to these two planners with ‘safety ensured’ and ‘only NN’, respectively.

Table II shows the performance of the neural network for behavior identification. We classify all simulation entries in the dataset into three classes based on the difference of accelerations under different behaviors, $\delta a_{x,f}^* = |a_{x,f,1}^* - a_{x,f,2}^*|$. It is classified as easy, medium or hard if $\delta a_{x,f}^* > 0.5$, $0.25 < \delta a_{x,f}^* \leq 0.5$ or $\delta a_{x,f}^* \leq 0.25$, respectively. We conduct sensitivity analysis over the threshold a_{th} . It shows that with larger a_{th} , the uncertain rate is higher and error rate is lower for all three different difficulty levels. It meets our expectation because a larger a_{th} results in a more robust and conservative predictor, which is prone to be uncertain when it is less confident. It also presents that for easy cases, the performance can be considerably great because a larger $\delta a_{x,f}^*$ means that it is more distinguishable.

We then evaluate the statistical performance of our planner framework through extensive simulations, as shown in table III. First we have four classes, ‘only NN, non-collaborative’, ‘safety ensured, non-collaborative’, ‘only NN, collaborative’ and ‘safety ensured, collaborative’, to compare the performance of our ‘safety ensured’ planner and the ‘only NN’ planner when the following vehicle is collaborative or not. Then under each class, we have four sub-classes with different experimental settings, which indicate the ranges that $a_{x,l}$ and δp will uniformly sample from. δp is the initial longitudinal distance between leading vehicle and ego vehicle. Thus $-6 \leq a_{x,l} \leq 4$ and $7 \leq \delta p \leq 37$ correspond to easier lane changing scenarios, while $-6 \leq a_{x,l} \leq 0$ and $7 \leq \delta p \leq 17$ correspond to more congested and dangerous scenarios. For each sub-class, we conduct one million simulations with randomly generated relative positions, velocities and IDM parameters.

For every round simulation with a horizon of ten seconds, the ego vehicle attempts to change lanes until it collides

TABLE III
SAFETY AND PERFORMANCE EVALUATION FOR THE PLANNER FRAMEWORK

	experimental setting	collision rate	success rate	lane changing time	final lateral position
only NN, non-collaborative	$-6 \leq a_{x,l} \leq 4, 7 \leq \delta p \leq 37$	9.57%	52.57%	1.741 s	2.444 m
	$-6 \leq a_{x,l} \leq 0, 7 \leq \delta p \leq 37$	15.93%	21.06%	1.735 s	1.115 m
	$-6 \leq a_{x,l} \leq 4, 7 \leq \delta p \leq 17$	26.59%	52.52%	1.758 s	2.902 m
	$-6 \leq a_{x,l} \leq 0, 7 \leq \delta p \leq 17$	44.18%	20.98%	1.753 s	1.447 m
safety ensured, non-collaborative	$-6 \leq a_{x,l} \leq 4, 7 \leq \delta p \leq 37$	0%	52.42%	1.752 s	2.287 m
	$-6 \leq a_{x,l} \leq 0, 7 \leq \delta p \leq 37$	0%	20.82%	1.777 s	1.064 m
	$-6 \leq a_{x,l} \leq 4, 7 \leq \delta p \leq 17$	0%	52.07%	1.793 s	2.331 m
	$-6 \leq a_{x,l} \leq 0, 7 \leq \delta p \leq 17$	0%	20.23%	1.883 s	1.140 m
only NN, collaborative	$-6 \leq a_{x,l} \leq 4, 7 \leq \delta p \leq 37$	11.26%	52.58%	1.737 s	2.503 m
	$-6 \leq a_{x,l} \leq 0, 7 \leq \delta p \leq 37$	18.75%	21.08%	1.733 s	1.174 m
	$-6 \leq a_{x,l} \leq 4, 7 \leq \delta p \leq 17$	28.38%	52.55%	1.751 s	2.973 m
	$-6 \leq a_{x,l} \leq 0, 7 \leq \delta p \leq 17$	47.16%	21.02%	1.749 s	1.520 m
safety ensured, collaborative	$-6 \leq a_{x,l} \leq 4, 7 \leq \delta p \leq 37$	0%	52.56%	1.737 s	2.318 m
	$-6 \leq a_{x,l} \leq 0, 7 \leq \delta p \leq 37$	0%	21.04%	1.737 s	1.114 m
	$-6 \leq a_{x,l} \leq 4, 7 \leq \delta p \leq 17$	0%	52.48%	1.754 s	2.346 m
	$-6 \leq a_{x,l} \leq 0, 7 \leq \delta p \leq 17$	0%	20.90%	1.761 s	1.162 m

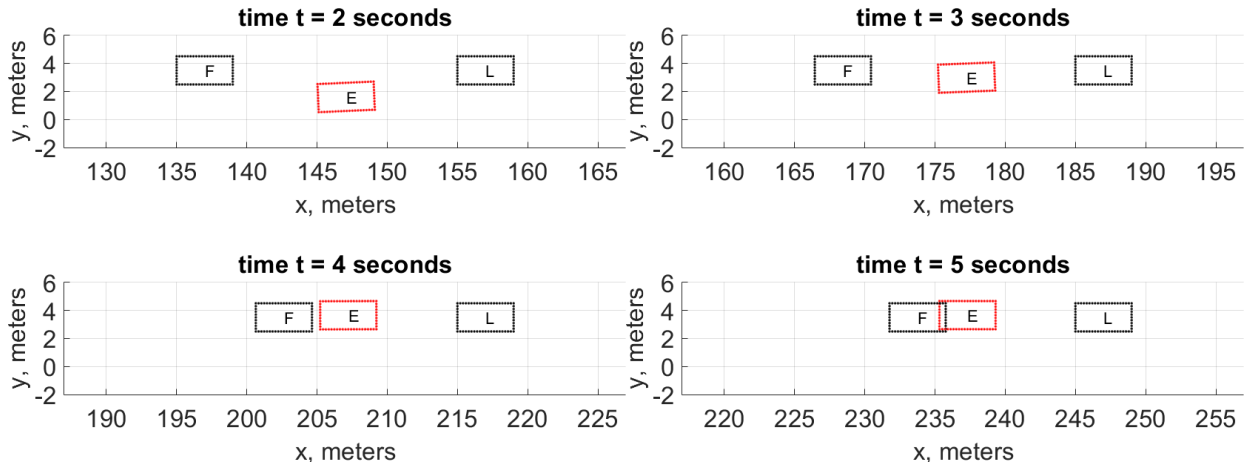


Fig. 6. The x and y axes show the longitudinal and lateral positions of vehicles. Four subplots show the positions at different times. Red rectangle represents the ego vehicle, and black rectangles are surrounding vehicles. It corresponds to the scenario that initial velocity is 30 m/s for all vehicles, and the distance between leading and following vehicle is 20 m. The following vehicle accelerates at $t = 2$ seconds to prevent the ego vehicle from cutting in. The ego vehicle is controlled by the ‘only NN’ planner.

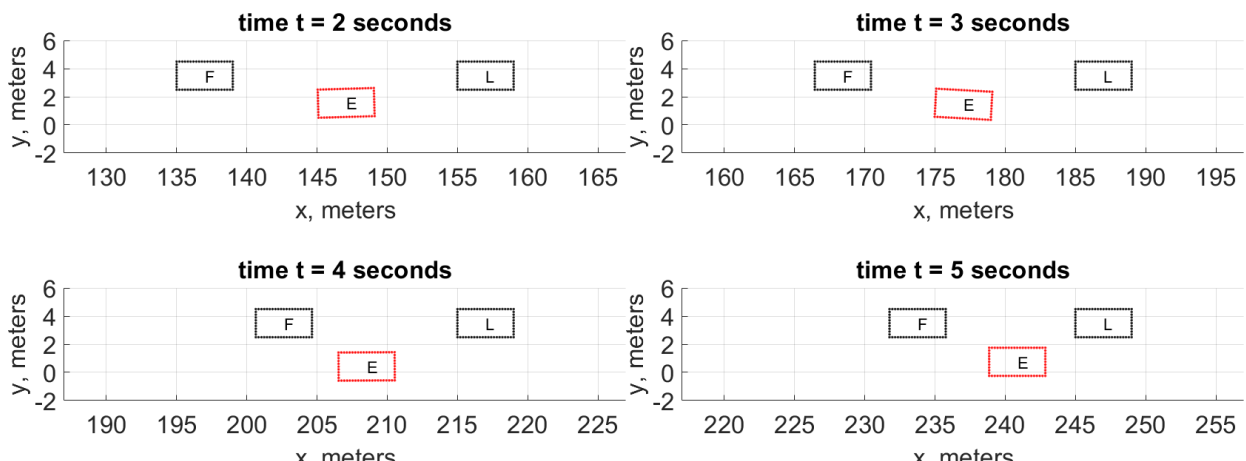


Fig. 7. The x and y axes show the longitudinal and lateral positions of vehicles. Four subplots show the positions at different times. Red rectangle represents the ego vehicle, and black rectangles are surrounding vehicles. It corresponds to the same scenario as in Fig. 6, except that the ego vehicle is controlled by the ‘safety ensured’ planner.

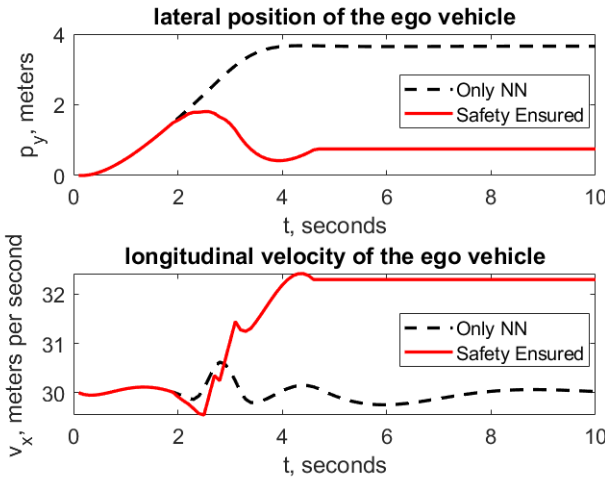


Fig. 8. Lateral position and longitudinal velocity of the ego vehicle in the same scenario as in Fig. 6.

with other vehicles. It is successful if the ego vehicle finally crosses the border of two lanes within the simulation horizon without any collision. For all successful lane changing simulations, we compute the average time that it takes to cross the border. For all safe simulations, we compute the average of final lateral positions. The lateral position $y = 3.5$ meters represents the center of target lane, and $y = 1.75$ meters is the border of two lanes.

Table III presents that: (1) our planner design ‘safety ensured’ results in zero collision rate in all simulations whenever the following vehicle is collaborative or not, while ‘only NN’ leads to a positive collision rate, especially in more challenging scenarios. (2) under ‘only NN’, the ego vehicle has a slightly higher lane changing success rate, less lane changing time and larger final lateral position. However, these advantages are almost negligible compared with ‘safety ensured’ planner. (3) generally speaking, when following vehicle is collaborative, we can have higher success rate, less lane changing time and larger final lateral position.

We further demonstrate the strength of our ‘safety ensured’ planner with an example. The initial longitudinal velocities of all three vehicles are set to 30 meters per second. The distance between leading and following vehicle is 20 meters. Then we let the following vehicle start accelerating with $a_{x,f} = 4$ meters per second squared until $p_{x,l} - p_{x,f} \leq 17$ meters at $t = 2$ seconds. Then it adjusts velocity and attempts to maintain the distance to the leading vehicle. Fig. 6 and 7 present the relative position changes of vehicles when the ego vehicle is controlled by ‘only NN’ and ‘safety ensured’ planners, respectively. Under the ‘only NN’ planner, the ego vehicle completes lane changing at $t = 3$ seconds, but collides with the following vehicle at $t = 5$ seconds. Our ‘safety ensured’ planner prevents the collision proactively. As shown in Fig. 7, the ego vehicle aborts changing lanes at around $t = 3$ seconds, then hesitates around $y = 1$ meters and looks for the next chance to change lanes. Fig. 8 shows the lateral position and longitudinal velocity of the ego vehicle in the

simulation horizon.

V. CONCLUSION

In this work, we present a neural network based lane changing planner that can ensure safety even when the leading vehicle decelerates abruptly and the following vehicle accelerates aggressively in the target lane. We improve system efficiency and lane changing success rate in dense traffic by identifying the behavior intention of the following vehicle in real time. By considering both the steering and braking capability, the ego vehicle can attempt to change lanes as long as there exists a safe evasion trajectory. Through extensive simulations, we show that our ‘safety ensured’ planner results in no collision under comprehensive experimental settings, while sustaining the system performance, compared with the ‘only NN’ planner.

REFERENCES

- [1] M. Cheng, C. Yin, J. Zhang, S. Nazarian, J. Deshmukh, and P. Bogdan, “A general trust framework for multi-agent systems,” in *Proceedings of the 20th International Conference on Autonomous Agents and MultiAgent Systems*, 2021, pp. 332–340.
- [2] Z. Cao, E. Biyik, W. Z. Wang, A. Raventos, A. Gaidon, G. Rosman, and D. Sadigh, “Reinforcement learning based control of imitative policies for near-accident driving,” *arXiv preprint arXiv:2007.00178*, 2020.
- [3] K. B. Naveed, Z. Qiao, and J. M. Dolan, “Trajectory planning for autonomous vehicles using hierarchical reinforcement learning,” *arXiv preprint arXiv:2011.04752*, 2020.
- [4] M. S. Nosrati, E. A. Abolfathi, M. Elmahioui, P. Yadollahi, J. Luo, Y. Zhang, H. Yao, H. Zhang, and A. Jamil, “Towards practical hierarchical reinforcement learning for multi-lane autonomous driving,” 2018.
- [5] J. Li, L. Sun, M. Tomizuka, and W. Zhan, “A safe hierarchical planning framework for complex driving scenarios based on reinforcement learning,” *arXiv preprint arXiv:2101.06778*, 2021.
- [6] J. Wang, Y. Wang, D. Zhang, Y. Yang, and R. Xiong, “Learning hierarchical behavior and motion planning for autonomous driving,” *arXiv preprint arXiv:2005.03863*, 2020.
- [7] H. Ma, J. Chen, S. E. Li, Z. Lin, Y. Guan, Y. Ren, and S. Zheng, “Model-based constrained reinforcement learning using generalized control barrier function,” *arXiv preprint arXiv:2103.01556*, 2021.
- [8] H.-D. Tran, F. Cai, M. L. Diego, P. Musau, T. T. Johnson, and X. Koutsoukos, “Safety verification of cyber-physical systems with reinforcement learning control,” *ACM Transactions on Embedded Computing Systems (TECS)*, vol. 18, no. 5s, pp. 1–22, 2019.
- [9] C. Huang, J. Fan, W. Li, X. Chen, and Q. Zhu, “Reachnn: Reachability analysis of neural-network controlled systems,” *ACM Transactions on Embedded Computing Systems (TECS)*, vol. 18, no. 5s, pp. 1–22, 2019.
- [10] R. Ivanov, J. Weimer, R. Alur, G. J. Pappas, and I. Lee, “Verisig: verifying safety properties of hybrid systems with neural network controllers,” in *Proceedings of the 22nd ACM International Conference on Hybrid Systems: Computation and Control*, 2019, pp. 169–178.
- [11] D. González, J. Pérez, V. Milanés, and F. Nashashibi, “A review of motion planning techniques for automated vehicles,” *IEEE Transactions on Intelligent Transportation Systems*, vol. 17, no. 4, pp. 1135–1145, 2015.
- [12] C. Katrakazas, M. Quddus, W.-H. Chen, and L. Deka, “Real-time motion planning methods for autonomous on-road driving: State-of-the-art and future research directions,” *Transportation Research Part C: Emerging Technologies*, vol. 60, pp. 416–442, 2015.
- [13] Z. Zheng, “Recent developments and research needs in modeling lane changing,” *Transportation research part B: methodological*, vol. 60, pp. 16–32, 2014.
- [14] Y. Luo, Y. Xiang, K. Cao, and K. Li, “A dynamic automated lane change maneuver based on vehicle-to-vehicle communication,” *Transportation Research Part C: Emerging Technologies*, vol. 62, pp. 87–102, 2016.

- [15] D. Yang, S. Zheng, C. Wen, P. J. Jin, and B. Ran, "A dynamic lane-changing trajectory planning model for automated vehicles," *Transportation Research Part C: Emerging Technologies*, vol. 95, pp. 228–247, 2018.
- [16] S. Sivaraman and M. M. Trivedi, "Dynamic probabilistic drivability maps for lane change and merge driver assistance," *IEEE Transactions on Intelligent Transportation Systems*, vol. 15, no. 5, pp. 2063–2073, 2014.
- [17] A. Talebpour, H. S. Mahmassani, and S. H. Hamdar, "Modeling lane-changing behavior in a connected environment: A game theory approach," *Transportation Research Procedia*, vol. 7, pp. 420–440, 2015.
- [18] C. Burger, T. Schneider, and M. Lauer, "Interaction aware cooperative trajectory planning for lane change maneuvers in dense traffic," in *2020 IEEE 23rd International Conference on Intelligent Transportation Systems (ITSC)*. IEEE, 2020, pp. 1–8.
- [19] D. Isele, "Interactive decision making for autonomous vehicles in dense traffic," in *2019 IEEE Intelligent Transportation Systems Conference (ITSC)*. IEEE, 2019, pp. 3981–3986.
- [20] T. Awal, M. Murshed, and M. Ali, "An efficient cooperative lane-changing algorithm for sensor-and communication-enabled automated vehicles," in *2015 IEEE Intelligent Vehicles Symposium (IV)*. IEEE, 2015, pp. 1328–1333.
- [21] M. Bouton, A. Nakhaei, K. Fujimura, and M. J. Kochenderfer, "Cooperation-aware reinforcement learning for merging in dense traffic," in *2019 IEEE Intelligent Transportation Systems Conference (ITSC)*. IEEE, 2019, pp. 3441–3447.
- [22] S. Bae, D. Saxena, A. Nakhaei, C. Choi, K. Fujimura, and S. Moura, "Cooperation-aware lane change maneuver in dense traffic based on model predictive control with recurrent neural network," in *2020 American Control Conference (ACC)*. IEEE, 2020, pp. 1209–1216.
- [23] F. Ye, X. Cheng, P. Wang, C.-Y. Chan, and J. Zhang, "Automated lane change strategy using proximal policy optimization-based deep reinforcement learning," in *2020 IEEE Intelligent Vehicles Symposium (IV)*. IEEE, 2020, pp. 1746–1752.
- [24] T. Shi, P. Wang, X. Cheng, C.-Y. Chan, and D. Huang, "Driving decision and control for automated lane change behavior based on deep reinforcement learning," in *2019 IEEE Intelligent Transportation Systems Conference (ITSC)*. IEEE, 2019, pp. 2895–2900.
- [25] A. Alizadeh, M. Moghadam, Y. Bicer, N. K. Ure, U. Yavas, and C. Kurtulus, "Automated lane change decision making using deep reinforcement learning in dynamic and uncertain highway environment," in *2019 IEEE Intelligent Transportation Systems Conference (ITSC)*. IEEE, 2019, pp. 1399–1404.
- [26] Y. Chen, C. Dong, P. Palanisamy, P. Mudalige, K. Muelling, and J. M. Dolan, "Attention-based hierarchical deep reinforcement learning for lane change behaviors in autonomous driving," in *Proceedings of the IEEE/CVF Conference on Computer Vision and Pattern Recognition Workshops*, 2019, pp. 0–0.
- [27] M. Naumann, H. Königshof, and C. Stiller, "Provably safe and smooth lane changes in mixed traffic," in *2019 IEEE Intelligent Transportation Systems Conference (ITSC)*. IEEE, 2019, pp. 1832–1837.
- [28] S. Shalev-Shwartz, S. Shammah, and A. Shashua, "On a formal model of safe and scalable self-driving cars," *arXiv preprint arXiv:1708.06374*, 2017.
- [29] C. Pek, P. Zahn, and M. Althoff, "Verifying the safety of lane change maneuvers of self-driving vehicles based on formalized traffic rules," in *2017 IEEE Intelligent Vehicles Symposium (IV)*. IEEE, 2017, pp. 1477–1483.
- [30] R. Chandru, Y. Selvaraj, M. Bränström, R. Kianfar, and N. Murgovski, "Safe autonomous lane changes in dense traffic," in *2017 IEEE 20th International Conference on Intelligent Transportation Systems (ITSC)*. IEEE, 2017, pp. 1–6.
- [31] X. Liu, G. Zhao, N. Masoud, and Q. Zhu, "Trajectory Planning for Connected and Automated Vehicles: Cruising, Lane Changing, and Platooning," *SAE International Journal of Connected and Automated Vehicles*, Jan 2021, in press.
- [32] J. Li, L. Sun, W. Zhan, and M. Tomizuka, "Interaction-aware behavior planning for autonomous vehicles validated with real traffic data," in *Dynamic Systems and Control Conference*, vol. 84287. American Society of Mechanical Engineers, 2020, p. V002T31A005.
- [33] I. G. Jin and G. Orosz, "Optimal control of connected vehicle systems with communication delay and driver reaction time," *IEEE Transactions on Intelligent Transportation Systems*, vol. 18, no. 8, pp. 2056–2070, 2016.